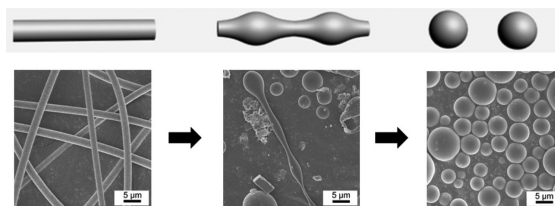


# Annealing Effect on Electrospun Polymer Fibers and Their Transformation into Polymer Microspheres

Ping-Wen Fan, Wan-Ling Chen, Ting-Hsien Lee, Jiun-Tai Chen\*

Electrospinning is a simple and convenient technique to produce polymer fibers with diameters ranging from several nanometers to a few micrometers. Different types of polymer fibers have been prepared by electrospinning for various applications. Among different post-treatment methods of electrospun polymer fibers, the annealing process plays a critical role in controlling the fiber properties. The morphology changes of electrospun polymer fibers under annealing, however, have been little studied. Here we investigate the annealing effect of electrospun poly(methyl methacrylate) (PMMA) fibers and their transformation into PMMA microspheres. PMMA fibers with an average size of 2.39  $\mu\text{m}$  are first prepared by electrospinning a 35 wt% PMMA solution in dimethylformamide. After the electrospun fibers are thermally annealed in ethylene glycol, a non-solvent for PMMA, the surfaces of the fibers undulate and transform into microspheres driven by the Rayleigh instability. The driving force of the transformation process is the minimization of the interfacial energy between the polymer fibers and ethylene glycol. The sizes of the microspheres fit well with the theoretical predictions. Longer annealing times are found to be required at lower temperatures to obtain the microspheres.



## 1. Introduction

In recent years, electrospinning has aroused considerable interest as a promising technique for producing polymer fibers with diameters ranging from several nanometers to a few micrometers.<sup>[1,2]</sup> Because of the high surface-area-to-volume ratios, electrospun polymer fibers have been investigated for a variety of applications such as catalysis,<sup>[3]</sup> filtration,<sup>[4]</sup> tissue engineering,<sup>[5]</sup> wound dressing,<sup>[6]</sup> and drug delivery.<sup>[7]</sup> These applications usually require different types of post-treatment after the preparation of the electrospun fibers. Among these post-treatment methods,

annealing is a useful process to control the properties of the polymer fibers. For example, Zong et al. reported that the crystallinity of electrospun poly(glycolide-co-lactide) was increased by annealing the samples at elevated temperatures without drawing.<sup>[8]</sup> They also found that the tensile strength of the electrospun membranes was greatly improved by stretching and annealing the samples. Liu et al. reported that the metastable gamma-crystals of as-spun nylon-6 fibers gradually melted and recrystallized into thermodynamically stable alpha-form crystals after annealing above 150 °C.<sup>[9]</sup> The annealing process is applied to not only electrospun polymer fibers, but also inorganic electrospun fibers, such as silica or titania. For example, Tomer et al. studied the erbia-modified electrospun titania nanofibers and found that an anatase titania crystal structure was obtained when the samples were annealed to 773 K, while a rutile phase was achieved when the samples were annealed to 1173 K.<sup>[10]</sup>

P. W. Fan, W. Chen, T. Lee, Prof. J. T. Chen  
Department of Applied Chemistry, National Chiao Tung  
University, Hsinchu, Taiwan 30050  
Tel: 886-3-5731631  
E-mail: jtchen@mail.nctu.edu.tw

Despite these works of annealing electrospun polymer fibers, the annealing effect on the morphology changes of electrospun polymer fibers has been little studied. Here we study the transformation process of electrospun polymer fibers under thermal annealing in ethylene glycol. Poly(methyl methacrylate) (PMMA) fibers are first prepared by electrospinning a solution of PMMA in dimethylformamide (DMF). The sizes and morphology of the PMMA fibers can be controlled by adjusting the electrospinning conditions, such as polymer concentration, applied voltage, and feeding rate. By thermally annealing the electrospun PMMA fibers in ethylene glycol, the surfaces of the fibers undulate and transform into polymer microspheres driven by the Rayleigh instability.

The Rayleigh instability is commonly seen in daily life. A simple example of the Rayleigh instability is a stream of water dripping from a faucet. The Rayleigh instability was pioneered by Plateau, who studied the instability in liquid cylinders.<sup>[11]</sup> He understood that the instability of these cylinders arises from the liquid surface tension. When the free surface of a liquid cylinder of radius  $R_0$  undulates with a wavelength  $\lambda$ , its surface area decreases, as long as  $\lambda$  is larger than the perimeter of the cylinder ( $2\pi R_0$ ). The distortion then amplifies and the liquid cylinder disintegrates into a chain of drops. Later, Rayleigh demonstrated that the wavelength of the distortion and the size of the drops are determined by the fastest distortion mode.<sup>[12]</sup> Similar calculations were further calculated by Nichols and Mullins, who extended Rayleigh's perturbation approach to solid cylinders.<sup>[13]</sup> They studied the mass transport of solid cylinders by either surface or volume diffusion. For an infinitely long cylinder of radius of  $R_0$  with an infinitesimal longitudinal sinusoidal perturbation, the perturbed surface is given by<sup>[13]</sup>

$$r = R_0 + \delta \sin(2\pi/\lambda)z \quad (1)$$

where  $\delta$  is the amplitude of the perturbation,  $\lambda$  is the wavelength of the perturbation, and  $z$  is the coordinate along the cylindrical axis. Nichols and Mullins calculated that the amplitude of a perturbation with a wavelength of  $\lambda > 2\pi R_0$  is expected to increase spontaneously with time, and the perturbations with  $\lambda_m = 2\pi\sqrt{2}R_0 = 8.89R_0$  have the maximum growth rate.<sup>[13]</sup> The solid cylinder then breaks up into a line of particles with an average spacing  $\lambda_m$  and diameter  $d = 3.78R_0$ . In their analysis, they assumed an isotropic surface energy of the initial solid cylinder. This assumption is violated in many cases, concerning the effect of anisotropic surface energy.<sup>[14]</sup>

The Rayleigh instability is commonly observed in metal nanowires. For example, Toimil-Molares et al. reported the Rayleigh instability in copper nanowires annealed at temperatures between 400 and 600 °C.<sup>[15]</sup> The copper nanowires fragment into chains of nanospheres, and the average diameter and spacing of the nanospheres

are in good agreement with theoretical predictions. The Rayleigh instability is also observed in polymer materials. For example, Park et al. studied that polymer strips on a silicon wafer rupture anisotropically upon thermal annealing, resulting in the formation of regularly spaced polymer drops.<sup>[16]</sup> Chen et al. also reported the Rayleigh instability in thin PMMA films confined within nanoporous alumina membranes.<sup>[17,18]</sup> After thermal annealing, the PMMA nanotubes undulate and eventually bridge across the cylindrical nanopore in the membrane, resulting in the formation of polymer nanorods with encapsulated holes.<sup>[17]</sup> For these experimental studies on the Rayleigh instability, the materials are usually placed on substrates during the annealing process. Consequently, the instability results are perturbed by the interactions between the materials and the underlying substrates. For a film of liquid on a substrate, it may be in the complete wetting or the partial wetting regimes, depending on the spreading coefficient, which is measured by the interfacial energy difference between the bare substrate and the substrate covered with a film of liquid.<sup>[19]</sup> These different wetting regimes strongly affect the results of the transformation of materials driven by the Rayleigh instability.<sup>[20]</sup> Therefore, it is necessary to prevent the substrate effect during the annealing process.

In order to study the annealing effect of electrospun PMMA fibers driven by the Rayleigh instability and to avoid the substrate effect, here we anneal PMMA fibers dispersed in ethylene glycol. Ethylene glycol is a non-solvent for PMMA and provides an environment for annealing the fibers uniformly. The only interface that needs to be considered is between the polymer and ethylene glycol, and no substrate is involved in the annealing process. We find that the electrospun polymer fibers undulate and transform into spheres upon annealing. This method for making polymer spheres is different from other traditional methods such as the reprecipitation method.<sup>[21]</sup> In addition, the sizes of the polymer spheres are in agreement with theoretical predictions. The kinetics of the transformation process is found to depend on the annealing conditions such as the annealing temperature or the annealing time. For higher annealing temperatures, shorter times are necessary for transforming the electrospun polymer fibers into spheres.

## 2. Experimental Section

### 2.1. PMMA Fibers by Electrospinning

PMMA ( $\bar{M}_w$ : 75 kg mol<sup>-1</sup>) was obtained from Sigma Aldrich. DMF was obtained from Tedia. Ethylene glycol was purchased from Scharlab. In a typical electrospinning experiment, a PMMA solution (35 wt%) in DMF was added into a syringe connected to a capillary nozzle with an inner diameter of 0.41 mm. The capillary

nozzle was connected to a high-voltage power supply (SIMCO), with a voltage range of 10–30 kV. The working distance between the capillary nozzle and the grounded collector was 10–20 cm. A syringe pump (KD Scientific) was used to feed the polymer solution at a constant flow rate ( $1 \text{ mL h}^{-1}$ ). The electrospinning process was performed at room temperature in a vertical spinning configuration.

## 2.2. Annealing Process of Electrospun PMMA Fibers

After the electrospun PMMA fibers were collected, they were placed in a 10 mL round-bottom flask containing 4 mL of ethylene glycol which was preheated to a desired temperature. A magnetic stir bar was used to agitate the solution at a constant speed of 200 rpm during the annealing process. After the samples were annealed for the desired periods of time (3 min to 3 h), the samples were filtered and washed with deionized water, followed by a drying process using a vacuum pump.

## 2.3. Structural Characterization

The glass temperatures ( $T_g$ ) of the polymers were measured by differential scanning calorimetry (DSC) using a SEIKO Instruments EXSTAR 6000 DSC. The samples before and after thermal annealing were characterized using a JEOL JSM-7401F scanning electron microscope at an accelerating voltage of 10 kV. Before the scanning electron microscopy (SEM) measurement, the samples were coated with 4 nm of platinum.

## 3. Results and Discussion

Figure 1 shows a schematic illustration of the fabrication process of electrospun PMMA fibers and PMMA microspheres. The whole process includes two main steps. The first step is to produce PMMA fibers by electrospinning. The

second step is to thermally anneal the PMMA fibers in ethylene glycol. In the electrospinning process, a PMMA solution is pumped through a nozzle at which a high voltage is applied relative to a grounded collector. A droplet is held by its surface tension at the end of the nozzle that is subjected to the electric field. As the intensity of the electric field is increased, the hemispherical shape of the droplet is destabilized by the accumulated charges on the droplet surface, and is elongated to form a conical shape known as the Taylor cone.<sup>[22]</sup> When the electric field reaches a critical value at which the repulsive force attributable to the electric field overcomes the surface tension force of the droplet, a charged jet of the solution is ejected from the tip of the Taylor cone. Upon fast evaporation of the solvent, the solution jet solidifies and dried fibers are deposited on the collector.

After the electrospinning process, the PMMA fibers are annealed in a flask containing ethylene glycol which is preheated to a desired temperature. Ethylene glycol is chosen because it has a high boiling point ( $197.3 \text{ }^\circ\text{C}$ ) and is a non-solvent for PMMA. By dispersing the fibers in ethylene glycol, the fibers are annealed uniformly and the aggregation of the fibers is effectively prevented. During the annealing process, the aggregation of the fibers is also prevented by stirring the mixture, a critical step in this study. Without stirring, the fibers aggregate and form a bulk PMMA film after the annealing process. We find that the stirring speed has no appreciable effect on the transformation process once the stirring speed is high enough to keep the fibers well dispersed in ethylene glycol. For all experiments discussed here, the stirring speed is fixed at 200 rpm. After the samples are annealed in ethylene glycol for different times, the samples are washed and filtered, followed by a drying process using a vacuum pump before conducting the SEM analysis.

Electrospinning is a simple and versatile technique to prepare polymer fibers. The morphology and sizes of the as-spun fibers are controlled by adjusting the experimental factors, such as polymer concentration, molecular weight, applied voltage, feeding rate, and working distance.<sup>[23]</sup> The SEM images of the PMMA ( $\bar{M}_w$ :  $75 \text{ kg mol}^{-1}$ ) fibers electrospun under different conditions are shown in the Supporting Information. One of the most common ways to control the sizes and morphology of the electrospun fibers is to adjust the feeding rate of the polymer solution.<sup>[24]</sup> In general, the fiber diameters are observed to increase with the feeding rate, and the fibers with smallest diameters are obtained at the lowest feeding

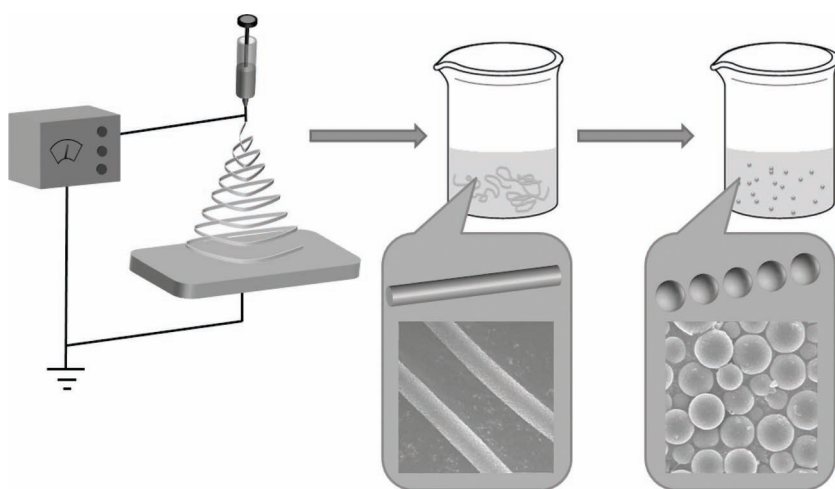


Figure 1. Schematic illustration of the fabrication process of electrospun PMMA fibers and PMMA microspheres. The PMMA fibers are first generated by electrospinning and transform into microspheres after they are annealed in ethylene glycol.

rate, in which the production rates are the lowest. Fridrich et al. showed that the charge density on the polymer jet is decreased exponentially by increasing the feeding rate, resulting in the weaker electrical force and larger diameters of fibers.<sup>[25]</sup> When the feeding rate is too fast, beaded fibers are also observed.

Another common way to control the diameters of the electrospun fibers is by changing the concentration of the polymer solution. A stable polymer jet is not maintained if the polymer concentration is lower than a critical value, because of the lower viscosity. For the case of lower polymer concentrations, polymer liquid jets may break into droplets and polymer fibers are unable to form.<sup>[26]</sup> Beads-on-string structures are also observed caused by the contraction of the jet and the entanglement of polymer chains at lower polymer concentrations.<sup>[27]</sup> It has been reported that the size of the beads and the distance between beads increases with the viscosity of the solution.<sup>[27]</sup> The beaded defects disappear as the polymer concentration is higher than a critical value. In general, the diameter of the electrospun polymer fiber increases as the polymer concentration increases. But the polymer solution might be difficult to be ejected from the capillary nozzle when the polymer concentration is too high because of the increased viscosity. In addition to the polymer concentration, the solution viscosity is also affected by the molecular weight of the polymers.<sup>[28]</sup>

The diameters and morphology of the polymer fibers can be controlled by other electrospinning conditions such as the applied voltage. With a higher applied voltage, the electric field is stronger, resulting in electrospun fibers with smaller diameters.<sup>[29]</sup> The morphology of the electrospun fibers is also strongly influenced by the dielectric constant of the solvent. A polymer solution with a high dielectric constant can prevent the bead formation and reduce the diameters of the fibers.<sup>[28]</sup> Here we use DMF as the solvent for making the PMMA solution. DMF has a high dielectric constant ( $\epsilon = 36.7$ ) and is commonly used as solvent for electrospinning PMMA fibers.

For the annealing studies, we used the polymer fibers fabricated by the same electrospinning conditions. The PMMA fibers are electrospun at the applied voltage of 10 kV with a working distance of 20 cm from 35% PMMA ( $\bar{M}_w$ : 75 kg mol<sup>-1</sup>) solution in DMF at a feeding rate of 1 mL h<sup>-1</sup>. We choose electrospun fibers under these conditions because of their suitable sizes and stable fiber structures. The average diameter of the PMMA fibers electrospun under these conditions is  $\sim 2.39 \mu\text{m}$  with a standard

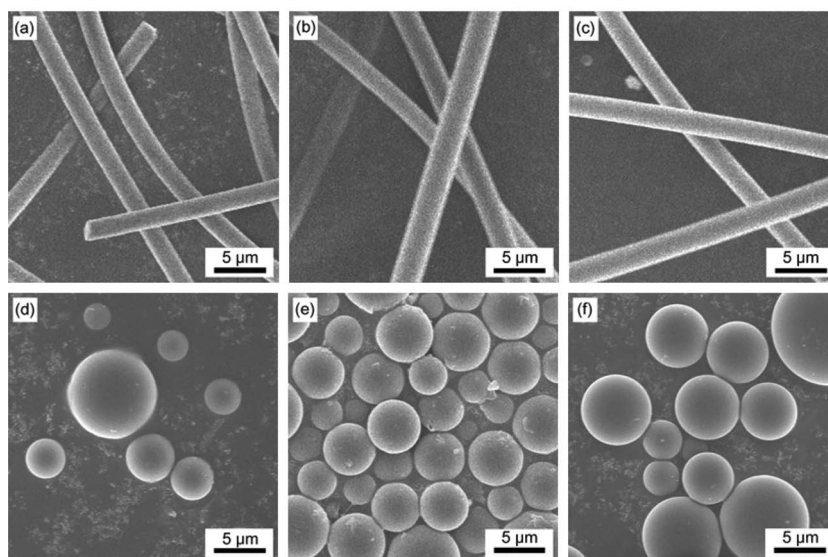


**Figure 2.** SEM images of electrospun PMMA fibers annealed in ethylene glycol for 3 h at different temperatures: (a) room temperature, (b) 80, (c) 90, (d) 120, (e) 130, and (f) 140 °C.

deviation of 0.45  $\mu\text{m}$ . The size distribution of the as-spun PMMA fibers is shown in the Supporting Information.

The electrospun PMMA fibers are annealed in ethylene glycol for different periods of time at different temperatures to investigate the kinetics of the structure transformation resulting from the Rayleigh instability. Figure 2 shows the results of electrospun PMMA fibers annealed in ethylene glycol at different temperatures for 3 h. The fiber structures are retained when the polymer fibers are annealed at room temperature, as shown in Figure 2a. If the fibers are annealed at higher temperatures but below the glass transition of PMMA ( $T_g$  of PMMA: 106 °C, measured by DSC), the fibril morphology is still observed. Although there have been many reports on the interface and surface effects on the glass transition temperatures in polymer thin films,<sup>[30,31]</sup> here we only consider the  $T_g$  of the bulk polymer, because the polymer fibers are not deposited on a substrate and the sizes of the fibers are in the micrometer range. When the samples are annealed at temperatures higher than the  $T_g$  of the polymers, transformation from fibers to microspheres is observed. Figure 2d–f show the microspheres annealed for 3 h at 120, 130, and 140 °C, respectively.

To understand more about the transformation process of the fibers into microspheres, we study the electrospun fibers annealed at the same temperature for different periods of time. When the electrospun PMMA fibers are annealed at 120 °C, the fiber shapes are retained at a shorter annealing time (0–15 min). At a longer annealing time (45 min), an intermediate state is observed (see Figure S3, Supporting Information). When the fibers are annealed for 3 h, all fibers are transformed into microspheres. At higher annealing temperatures, the structural

transformation is found to occur more rapidly because of the lower melt viscosity, where PMMA fibers were annealed at 140 °C for different periods of time (see Figure S4, Supporting Information). When the Rayleigh instability is applied to viscoelastic materials, the viscosity resists the breakup of the fluid jet and the characteristic time for the fastest growing mode of the jet breakup is

$$\tau_m = \eta R_0 / \sigma \quad (2)$$

where  $\tau_m$  is the characteristic time,  $\eta$  is the viscosity,  $R_0$  is the original radius, and  $\sigma$  is the surface tension of the interface.<sup>[32]</sup> Thus,  $\tau_m$  is proportional to the viscosity of the fluid and should decrease with increasing the annealing temperature, as we observe here.

To do a more quantitative study on the transformation process from electrospun fibers to microspheres, the sizes of the as-spun fibers are compared to the sizes of the microspheres. The sizes and morphology of the polymer structures annealed at different temperatures are summarized in Figure 3a. The average size of the as-spun PMMA fibers is 2.39  $\mu\text{m}$  with a standard deviation of 0.45  $\mu\text{m}$ . From the calculation by Nichols and Mullins based on the surface diffusion mechanism, the perturbations with  $\lambda_m = 8.89R_0$  have the maximum growth rate.<sup>[13]</sup> As the amplitudes of these perturbations increase, the solid cylinder breaks up into spheres with an estimated spacing of  $\lambda_m$  and a diameter  $d = 3.78R_0$ . By using 2.39  $\mu\text{m}$  as  $2R_0$ , the calculated

diameter of the microspheres is 4.52  $\mu\text{m}$ . Figure 3b shows a plot of the average diameters of the microspheres versus the annealing temperatures. Compared with the calculated value ( $d = 4.52 \mu\text{m}$ ), which is indicated by the dashed line in Figure 3b, the average sizes of the microspheres agree well with the theoretical calculations. Although the size distributions of microspheres annealed at different temperatures have some deviations (see Figure S5, Supporting Information), the average diameters are between 3.98 and 5.49  $\mu\text{m}$ , close to the calculated size. We conclude that the average diameters of microspheres are independent of the annealing temperatures, indicating that the polymer fibers undergo the same transformation pathways even at different annealing temperatures. The difference in the size distributions of the microspheres annealed at different temperatures might be caused by three factors: 1) the different size distributions of the as-spun fibers; 2) the different numbers of the counted samples at different annealing temperatures; and 3) the possibility that two or more microspheres might touch and merge together during the annealing process.

The graphical illustrations and SEM images of polymer fibers, undulated polymer structures, and polymer microspheres are shown in Figure 3c. The transformation and fragmentation processes are induced by the Rayleigh instability. The surface of the fiber undulates to decrease the interfacial energy between the polymer and ethylene

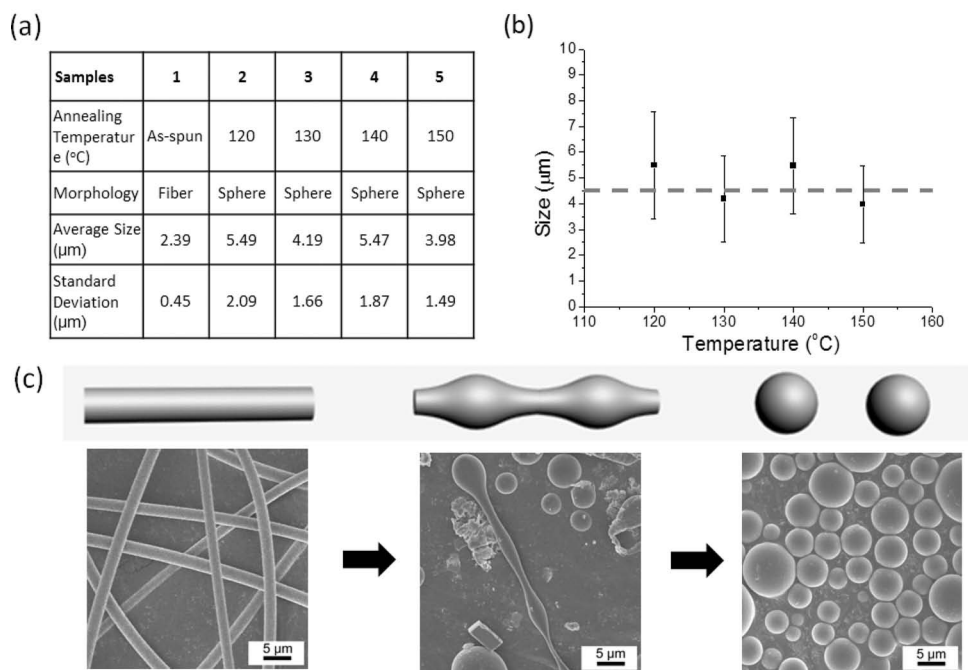


**Figure 3.** (a) A summary table of the polymer samples annealed at different temperatures. (b) A plot of the microsphere size versus the annealing temperature. The error bars represent the standard deviation. The dashed line indicates the calculated value of the microsphere size at 4.52  $\mu\text{m}$  predicted by the theoretical model. (c) Graphical illustrations and SEM images of polymer fibers, undulated polymer structures, and polymer microspheres.

glycol. As the amplitude of the undulation increases, the solid cylinder breaks up into a line of spheres. The SEM image for the undulated state is also shown in Figure 3c, which is obtained by annealing the sample at 130 °C for 30 min. We notice that the undulated structures are only present for a narrow range of annealing conditions, indicating that the fiber soon transforms into spheres once the undulation starts. After the transformation, the polymer sphere is at a stable state with the minimum interfacial energy between the polymer and ethylene glycol, unless a sphere touches with other spheres.

Strictly speaking, the calculation of the theoretical size of the polymer microspheres driven by the Rayleigh instability is based on the assumption that the total volumes of the polymers are conserved before and after the annealing processes. To test this assumption, first we consider the Hildebrand solubility parameters ( $\delta$ ) of PMMA and ethylene glycol. The Hildebrand solubility parameter is defined as the square root of the cohesive energy density and is a good indicator for solvation and swelling.<sup>[33]</sup> Polymers are dissolved in solvents with similar values of solubility parameters. The solubility parameter of PMMA is  $9.3 \text{ cal}^{1/2} \text{ cm}^{-3/2}$ , which is considerably different from the solubility parameter of ethylene glycol ( $\delta = 16.3 \text{ cal}^{1/2} \text{ cm}^{-3/2}$ ). Consequently, PMMA is not soluble in ethylene glycol and the total volume of the PMMA fibers is not affected during the annealing process. Another possible factor to consider for the volume change of the polymer fiber during the annealing process is the structure change induced by the chain recoiling. Pastor et al. reported the low shrinkage of poly(ethylene terephthalate) (PET) fibers during free-ends thermal annealing.<sup>[34]</sup> They reported that the conformation transition from trans to gauche causes chain coiling and loss of orientation of the chains of the PET fibers. In our study, the chain coiling process might also happen in the electrospun PMMA fibers during the thermal annealing process, resulting in the slight reduction of the total volume. But the volume change is expected to be ignored by comparing the small volume change with the total volume.

Putting all the results together, we obtain a phase diagram of the polymer structures annealed in ethylene glycol at different temperatures for different times. In Figure 4, the closed circles indicate that the fiber morphologies are retained, while the closed boxes indicate that the spherical morphologies are obtained. At higher annealing

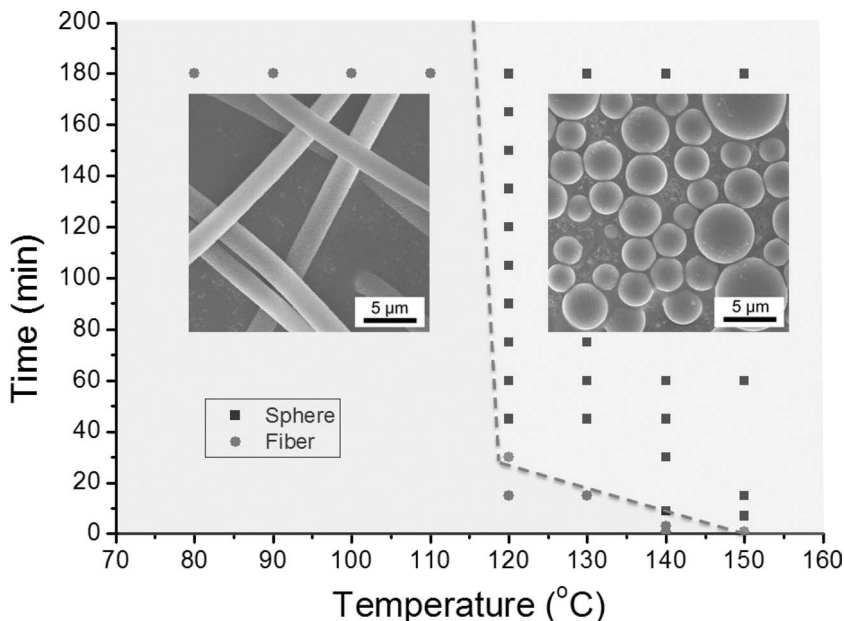


**Figure 4.** The schematic phase diagram of the polymer structures annealed in ethylene glycol at different temperatures for different times. The closed circles indicate that the fiber morphologies are retained, while the closed boxes indicate that the spherical morphologies are obtained.

temperatures, shorter times are required to transform the PMMA fibers into microspheres, which is predicted by Equation (2) which states a polymer melt with a lower viscosity has a shorter characteristic time. The transition is also indicated by the dashed line in Figure 4.

#### 4. Conclusion

In conclusion, we report the thermal annealing effect of electrospun PMMA fibers and their transformation into microspheres. The substrate effect is avoided by dispersing the fibers in ethylene glycol, a non-solvent for the polymer. In the annealing process, stirring is found to be critical to prevent aggregation of the fibers. Upon annealing, the surfaces of the PMMA fibers undulate and transform into microspheres driven by the Rayleigh instability. The sizes of the microspheres fit well with the theoretical predictions. The annealing times required for the transformation are shorter at higher temperatures, at which the viscosity of the polymer melt is lower. A simple phase diagram is also constructed for the fibers annealed at different temperatures and holding times.

Studies are currently being pursued to apply the transformation process of polymer fibers to other materials, such as electrospun titania or silica fibers. Possible future works also include the instability studies of polymer fibers composed of polymer blends or block copolymers. The phase separation behavior of multicomponent

polymers is expected to affect the kinetics of the instability phenomena, and interesting morphologies which have not been observed in the bulk state might also be shown.

## Supporting Information

Supporting Information is available from the Wiley Online Library or from the author.

Acknowledgements: This work was supported by the National Science Council.

Received: November 3, 2011; Revised: December 6, 2011; Published online: January 23, 2012; DOI:10.1002/marc.201100734

Keywords: annealing; interfacial tension; morphology; poly(methyl methacrylate);

- [1] D. Li, Y. N. Xia, *Adv. Mater.* **2004**, *16*, 1151.
- [2] A. Greiner, J. H. Wendorff, *Angew. Chem. Int. Ed.* **2007**, *46*, 5670.
- [3] Y. Q. Dai, W. Y. Liu, E. Formo, Y. M. Sun, Y. N. Xia, *Polym. Adv. Technol.* **2011**, *22*, 326.
- [4] S. Agarwal, J. H. Wendorff, A. Greiner, *Polymer* **2008**, *49*, 5603.
- [5] Q. P. Pham, U. Sharma, A. G. Mikos, *Tissue Eng.* **2006**, *12*, 1197.
- [6] A. Martins, R. L. Reis, N. M. Neves, *Int. Mater. Rev.* **2008**, *53*, 257.
- [7] N. Ashammakhi, I. Wimpenny, L. Nikkola, Y. Yang, *J. Biomed. Nanotechnol.* **2009**, *5*, 1.
- [8] X. H. Zong, S. F. Ran, D. F. Fang, B. S. Hsiao, B. Chu, *Polymer* **2003**, *44*, 4959.
- [9] Y. Liu, L. Cui, F. X. Guan, Y. Gao, N. E. Hedin, L. Zhu, H. Fong, *Macromolecules* **2007**, *40*, 6283.
- [10] V. Tomer, R. Teye-Mensah, J. C. Tokash, N. Stojilovic, W. Kataphinan, E. A. Evans, G. G. Chase, R. D. Ramsier, D. J. Smith, D. H. Reneker, *Sol. Energy Mater. Sol. Cells* **2005**, *85*, 477.
- [11] J. Plateau, *Transl. Annu. Rep. Smithsonian Inst.* **1873**, 1863.
- [12] L. Rayleigh, *Proc. London Math. Soc.* **1878**, *10*, 4.
- [13] F. A. Nichols, W. W. Mullins, *Trans. Met. Soc. AIME* **1965**, *233*, 1840.
- [14] K. F. Gurski, G. B. McFadden, *Proc. R. Soc. London Ser. A-Math. Phys. Eng. Sci.* **2003**, *459*, 2575.
- [15] M. E. Toimil-Molares, A. G. Balogh, T. W. Cornelius, R. Neumann, C. Trautmann, *Appl. Phys. Lett.* **2004**, *85*, 5337.
- [16] J. Park, K. Y. Suh, S. Seo, H. H. Lee, *J. Chem. Phys.* **2006**, *124*, 5.
- [17] J. T. Chen, M. F. Zhang, T. P. Russell, *Nano Lett.* **2007**, *7*, 183.
- [18] D. Chen, J. T. Chen, E. Glogowski, T. Emrick, T. P. Russell, *Macromol. Rapid Commun.* **2009**, *30*, 377.
- [19] P. G. Degennes, *Rev. Mod. Phys.* **1985**, *57*, 827.
- [20] S. Karim, M. E. Toimil-Molares, A. G. Balogh, W. Ensinger, T. W. Cornelius, E. U. Khan, R. Neumann, *Nanotechnology* **2006**, *17*, 5954.
- [21] X. Q. Shen, F. He, J. H. Wu, G. Q. Xu, S. Q. Yao, Q. H. Xu, *Langmuir* **2011**, *27*, 1739.
- [22] G. Taylor, *Proc. R. Soc. Lond. A* **1969**, *313*, 453.
- [23] Z. M. Huang, Y. Z. Zhang, M. Kotaki, S. Ramakrishna, *Compos. Sci. Technol.* **2003**, *63*, 2223.
- [24] J. T. Chen, W. L. Chen, P. W. Fan, *ACS Macro Lett.* **2012**, *1*, 41.
- [25] S. V. Fridrikh, J. H. Yu, M. P. Brenner, G. C. Rutledge, *Phys. Rev. Lett.* **2003**, *90*, 4.
- [26] M. M. Hohman, M. Shin, G. Rutledge, M. P. Brenner, *Phys. Fluids* **2001**, *13*, 2201.
- [27] H. Fong, I. Chun, D. H. Reneker, *Polymer* **1999**, *40*, 4585.
- [28] W. K. Son, J. H. Youk, T. S. Lee, W. H. Park, *Polymer* **2004**, *45*, 2959.
- [29] C. Wang, C. H. Hsu, J. H. Lin, *Macromolecules* **2006**, *39*, 7662.
- [30] J. A. Forrest, K. Dalnoki-Veress, J. R. Stevens, J. R. Dutcher, *Phys. Rev. Lett.* **1996**, *77*, 2002.
- [31] J. A. Forrest, K. Dalnoki-Veress, J. R. Dutcher, *Phys. Rev. E* **1997**, *56*, 5705.
- [32] K. V. Edmond, A. B. Schofield, M. Marquez, J. P. Rothstein, A. D. Dinsmore, *Langmuir* **2006**, *22*, 9052.
- [33] B. A. Miller-Chou, J. L. Koenig, *Prog. Polym. Sci.* **2003**, *28*, 1223.
- [34] J. C. Rodriguez Cabello, J. Santos, J. C. Merino, J. M. Pastor, *J. Polym. Sci., Part B: Polym. Phys.* **1996**, *34*, 1243.